



Published in final edited form as:

*Glia*. 2012 January ; 60(1): 83–95. doi:10.1002/glia.21250.

## Local disruption of glial adenosine homeostasis in mice associates with focal electrographic seizures: a first step in epileptogenesis?

Tianfu Li, Nikki Lytle, Jing-Quan Lan, Ursula S. Sandau, and Detlev Boison\*

Robert S. Dow Neurobiology Laboratories, Legacy Research Institute, Portland, Oregon 97232, USA

### Abstract

Astrogliosis and associated dysfunction of adenosine-homeostasis are pathological hallmarks of the epileptic brain and thought to contribute to seizure generation in epilepsy. We hypothesized that astrogliosis – an early component of the epileptogenic cascade – might be linked to focal seizure onset. To isolate the contribution of astrogliosis to ictogenesis from other pathological events involved in epilepsy, we used a minimalistic model of epileptogenesis in mice, based on a focal onset status epilepticus triggered by intraamygdaloid injection of kainic acid. We demonstrate acute neuronal cell loss restricted to the injected amygdala and ipsilateral CA3, followed three weeks later by focal astrogliosis and overexpression of the adenosine-metabolizing enzyme adenosine kinase (ADK). Using synchronous electroencephalographic recordings from multiple depth electrodes, we identify the KA-injected amygdala and ipsilateral CA3 as two independent foci for the initiation of non-synchronized electrographic subclinical seizures. Importantly, seizures remained focal and restricted to areas of ADK-overexpression. However, after systemic application of a non-convulsive dose of an adenosine A<sub>1</sub>-receptor antagonist, seizures in amygdala and CA3 immediately synchronized and spread throughout the cortex, leading to convulsive seizures. This focal seizure phenotype remained stable over at least several weeks. We conclude that astrogliosis via disruption of adenosine homeostasis *per se* and in the absence of any other overt pathology, is associated with the emergence of spontaneous recurrent subclinical seizures, which remain stable over space and time. A secondary event, here mimicked by brain-wide disruption of adenosine signaling, is likely required to turn pre-existing subclinical seizures into a clinical seizure phenotype.

### Keywords

Adenosine kinase; astrogliosis; epilepsy; amygdala; CA3

### INTRODUCTION

Astrogliosis is a pathological hallmark of the epileptic brain (Binder and Steinhauser 2006) and recent findings from several laboratories suggest an astrocytic basis for epilepsy (Seifert et al. 2010). Astrocytes can impair homeostatic control of network excitability in epilepsy through multiple mechanisms such as impaired K<sup>+</sup>-buffering (Hinterkeuser et al. 2000), dysfunctional gap junctions (Rouach et al. 2008), dysfunctional glutamate homeostasis (Eid

\*Corresponding author: Detlev Boison, Robert S. Dow Neurobiology Laboratories, Legacy Research Institute, 1225 NE 2<sup>nd</sup> Avenue, Portland, OR 97232, USA, Tel: +1 (503) 413-1754; Fax: +1 (503) 413-5465, dboison@downeurobiology.org.

et al. 2008), changes in calcium buffering and gliotransmitter release (Pascual et al. 2005), and dysfunctional adenosine homeostasis (Boison 2008).

The brain's endogenous anticonvulsant adenosine is a homeostatic bioenergetic network regulator (Boison et al. 2011) whose concentration is largely controlled by an astrocyte based adenosine cycle (Boison et al. 2010). A major source for extracellular adenosine is release of its precursor adenosine-5'-triphosphate (ATP) from astrocytes and subsequent extracellular cleavage (Pascual et al. 2005). The reuptake of adenosine through equilibrative nucleoside transporters (ENTs) is driven by intracellular phosphorylation of adenosine to adenosine-5'-monophosphate (AMP) by adenosine kinase (ADK), an enzyme that in adult brain is predominantly expressed in astrocytes (Studer et al. 2006). Previous work from our laboratory, using mice with engineered changes in ADK expression levels, has demonstrated (i) that the tone of ambient adenosine inversely relates to ADK expression levels (Shen et al. 2011), and (ii) that ADK expression levels determine the brain's susceptibility to ischemia- (Pignataro et al. 2007) and seizure- (Li et al. 2008b) induced neuronal cell loss.

The ADK hypothesis of epileptogenesis (Boison 2008) is based on findings that astrogliosis in rodent models of epilepsy is associated with overexpression of ADK, resulting adenosine deficiency, and spontaneous electrographic subclinical seizures (Li et al. 2008b). This suggests that astrogliosis, caused by disruption of adenosine homeostasis, contributes to seizure generation and therefore implies that adenosine deficiency is a pathological hallmark of the epileptic brain (Boison 2008). Consequently, focal augmentation of adenosine signaling, e.g. by intracerebral implants of adenosine-releasing devices (Wilz et al. 2008), is highly effective in preventing seizures. Overexpression of ADK has recently been confirmed in sclerotic hippocampi resected from patients with temporal lobe epilepsy suggesting that adenosine dysfunction is likewise a pathological hallmark of human epilepsy (Aronica et al. 2011).

Although the evidence mentioned above provides a strong link between astrogliosis, ADK overexpression, and spontaneous seizures in epilepsy, it remains unclear whether astrogliosis with overexpression of ADK associates with the focal origin of recurrent seizure activity. To address our hypothesis that astrogliosis accompanied by adenosine dysfunction is an early component of the epileptogenic cascade and associated with the focal origin of seizure activity, several requirements needed to be met: (i) isolation of focal astrogliosis from other epileptogenic events commonly associated with epilepsy, such as mossy fiber sprouting, granule cell dispersion, hilar cell loss, or the emergence of ectopic neurons; (ii) simultaneous electroencephalographic (EEG) recordings from multiple depth electrodes to study at least two independent astrogliotic foci; and (iii) strategies to assess spatial and temporal spread of focal seizure activity. Here we used an intraamygdaloid injection of kainic acid in mice to model focal epileptogenesis (Li et al. 2008b); this is a minimalistic model of epilepsy in the sense that astrogliosis, overexpression of ADK, and spontaneous subclinical seizures all occur in the absence of other pathologies commonly associated with epilepsy (Li et al. 2008b). Using a combination of histology, synchronous EEG-recordings from multiple intracerebral leads, and pharmacology, we characterize two independent foci (in injured amygdala and ipsilateral CA3) comprised of astrogliosis and upregulated ADK that co-localize with the origin of focal subclinical seizure activity. We demonstrate that seizures between these two foci occur independent and are not synchronized based on the focal nature of adenosine deficiency. We further demonstrate that focal seizures appear stable over time whereas they rapidly synchronize and generalize once adenosine signaling is globally impaired in brain. Thus, astrogliosis, associated dysfunction in adenosine signaling, and focal onset of subclinical seizures might constitute an early event in the epileptogenic cascade.

## Materials and Methods

### Animal model

All experiments were carried out in an AAALAC-accredited facility in accordance to protocols approved by the Legacy Health Institutional Animal Care and Use Committee adhering to NIH regulations and guidelines on the humane use of animals in research. We adopted a mouse model of CA3-selective epileptogenesis that has been fully described (Li et al. 2008b) with modifications. Briefly, under anesthesia with 68.5% N<sub>2</sub>O, 30% O<sub>2</sub>, and 1.5% isoflurane, adult male C57BL/6 mice were affixed with 3 cortical electrodes (Plastics One Inc.) and a 26-gauge steel guide cannula (AP = -0.94 mm, ML = -2.85 mm from bregma) over the intact dura using dental cement. Anesthesia was discontinued and EEG recordings commenced. A 31-gauge internal cannula was inserted into the lumen of the guide (3.75 mm below the dura) and 0.3 µg KA in 0.2 µl PBS, pH 7.4, was injected into the amygdala. 30 min after KA injection, mice received lorazepam (6 mg/kg, i.v) to stop status epilepticus (SE). Control mice received an intraamygdaloid saline injection (0.2 µl). Three weeks or two months after KA or control injection, mice were implanted with bipolar coated stainless steel electrodes (80µm in diameter; Plastics One Inc.) in the ipsilateral CA1, CA3 and dentate gyrus (DG), or the ipsilateral CA3 and amygdala. Coordinates for the electrodes (relative to bregma) were CA3 (AP = -2.18 mm, L = -2.6 mm, DV = -2.6 mm), CA1 (AP = -2.18 mm, L = -2 mm, DV = -1.7 mm), DG (AP = -2.18 mm, L = -1.25 mm, DV = -2.15 mm), and amygdala (AP = 0.94 mm, L = 2.85 mm, DV = 4.25 mm). Two additional monopolar electrodes were placed onto the frontal cortex (to record cortical EEG) and cerebellum (as reference) in all animals. Electrodes were fixed with a pedestal of dental acrylate.

### Histology

For studies investigating the acute injury (24 h post KA) brains were harvested from 6 animals, frozen in 2-methylbutane (-30°C), and sectioned at 12 µm on a cryostat. Consecutive, coronal sections beginning at bregma -1.3 or -1.7 were collected for analysis of either the amygdala or hippocampus, respectively. The sections were processed for histopathology (Nissl staining using cresyl violet) or for detection of DNA fragmentation using the fluorescein-based terminal deoxynucleotidyl transferase (TdT)-mediated dUTP nick end-labeling (TUNEL) technique (Roche Molecular Biochemicals, Indianapolis, IN) as described (Li et al. 2008a; Li et al. 2008b). The TUNEL stained sections were also stained with DAPI (Invitrogen). Quantification was done for each animal by counting then averaging all TUNEL-positive cells in 3 adjacent brain sections for each region (the entire amygdala or CA1/3 field). Thus for each animal a total of 6 sections were analyzed.

For studies investigating chronic injury (either 3 weeks or 2 months after KA), 6 mice per time-point were transcardially perfused with 4% paraformaldehyde in PBS(0.15 M, pH 7.4). The brains were postfixed in the same fixative at 4°C for 6 h, cryoprotected in 10% DMSO in PBS (vol/vol), and cut into 40-µm coronal sections. Histochemistry was conducted in consecutive sections beginning at either bregma -1.3 or -1.7 for analysis of the amygdala and hippocampus, respectively. For the 3 week time-point, 2 serial sections separated by 80 µm were selected for Nissl staining with cresyl violet. Adjacent serial sections were selected for immunohistochemical detection of ADK and/or GFAP (2 sections per staining condition) according to our published procedures (Studer et al. 2006).

Astrogliosis was quantified by manually counting the total number of GFAP positive cells within a 200 × 300 µm field that encompasses the entire CA3a region of the hippocampus and a portion of the affected amygdala. The analysis fields were centered over the respective sites of injury in the ipsilateral hemisphere and the corresponding regions in the contralateral

hemisphere. Two sections from each region (amygdala and CA3a) were analyzed using standard stereological rules: cells contacting the top and right boundaries of the analysis field were included in the total cell count while those contacting the bottom and left boundaries were omitted. The average number of GFAP positive cells within the CA3a and amygdala were determined in ipsilateral and contralateral hemisphere from  $n = 6$  animals. ADK expression in amygdala and CA3 was analyzed by densitometry using a Kodak imaging system. Levels of ADK in each analysis field were initially measured as arbitrary density units and subsequently expressed as a percent change from contralateral ADK measurement.

### Seizure monitoring

Electrical brain activity was monitored three weeks or two months after KA injection using the Nervus EEG Recording System connected with a Nervus magnus 32/8 Amplifier and filtered (high-pass filter 0.3 Hz cutoff, low-pass 100 Hz). Each EEG file was analyzed manually by an observer blinded to the animal's treatment. EEG-seizure activity was defined as high-amplitude rhythmic discharges that clearly represented a new pattern of tracing (repetitive spikes, spike-and wave discharges, and slow waves) that lasted at least 5 s. Epileptic events occurring with an interval less than 5 s without the EEG returning to baseline were defined as belonging to the same seizure. Each animal was subjected to continuous EEG monitoring from 10 am to 6 pm followed by an injection of the adenosine A<sub>1</sub> receptor antagonist 8-cyclopentyl- 1,3-dipropylxanthine (DPCPX, 1 mg/kg in 20% DMSO/saline, i.p.). EEG recordings continued for an additional 2 hours. During the combined 10 hour period of EEG monitoring, animals were continuously observed for behavioral seizures. Behavioral seizures were scored based on the Racine scale (Racine 1978).

### Statistical analysis

Quantitative data were analyzed using GraphPAD Prism software (GraphPAD Software, La Jolla, CA). The data were first subjected to a normality test and an equal variance test. All data that passed these two tests were subsequently analyzed as follows: comparison of two groups was performed with the Student's *t* test and datasets containing more than two groups were analyzed with one way ANOVA followed by Student-Newman-Keuls multiple test for individual means. The null hypothesis was rejected at the  $P = 0.05$  level for all analyses.

## Results

### Cell loss 24 h after SE is restricted to two distinct foci: the amygdala and CA3

Kainic acid induced SE is a well-known and frequently used trigger for subsequent epileptogenesis (Dudek et al. 2002). To isolate astrogliosis from histopathological alterations commonly associated with epilepsy, we chose the intraamygdaloid KA-model of focal onset SE with restricted duration (Li et al. 2008b). To provide a baseline for our subsequent investigations we first characterized the acute response to an intraamygdaloid injection of KA. A single intraamygdaloid injection of KA into adult male C57BL/6 mice resulted in SE comprised of multiple type IV cortical electrographic seizures, which are a characteristic of this injury paradigm. The type IV seizures had high-voltage, polyspike paroxysmal discharges of >1 Hz frequency and were terminated after 30 min by lorazepam (Fig. 1). Acute brain injury assessed 24 hours after the KA injection was characterized by focal injuries restricted to the amygdala and CA3 of the ipsilateral hippocampus (Fig. 2, Fig. 3), while other brain areas were devoid of any signs of injury (not shown). Profound focal cell loss in the ipsilateral amygdala became apparent by adisrupted Nisslstaining pattern with reduced intragranular bodies (Fig. 2B,D) and was confirmed by the presence of

TUNEL-positive cells ( $79.2 \pm 15.4$  cells per section;  $n = 6$  mice, 3 slices each; Fig. 2F). In contrast, neither the contralateral amygdala of injured mice (Fig. 2A,C,E) nor the ipsilateral amygdala of control injected mice (data not shown) displayed any signs of neuronal cell loss. In addition to the focal injury in the injected amygdala, KA injected mice were characterized by a second focal area of neuronal injury that was restricted to the ipsilateral CA3 and extended throughout the rostral-caudal extent of the hippocampus (Fig. 3A–D). This focal injury was associated with the profound appearance of TUNEL-positive cells ( $70.2 \pm 11.8$  cells per section at level of Fig. 3F;  $n = 6$  mice, 3 sections each). Furthermore, the TUNEL-positive cells within the ipsilateral CA3 had condensed nuclei (Fig. 3F, inset), as confirmed using a DAPI stain (Fig. 3J–M), which is a morphological feature indicative of apoptosis. High magnification DAPI images of injured cells within the CA3 revealed a concentrated staining pattern indicative of chromatin condensation (arrows; Fig. 3K, inset) compared to adjacent unaffected cells. In contrast to the injured hemisphere, no signs of any injury became evident in the contralateral hippocampus of KA injected animals as evidenced by Nissl (Fig. 3A), TUNEL, and DAPI staining (data not shown). In addition, intraamygdaloid saline injected control animals were devoid of any signs of injury. Together, our data demonstrate the existence of two discrete areas of focal injury, confined to the ipsilateral amygdala and CA3 subregion of the hippocampus, as a histopathological hallmark of our model.

### **Astrogliosis three weeks after SE is restricted to two distinct foci in amygdala and CA3 and accompanied by overexpression of ADK**

In order to selectively study the contribution of astrogliosis to seizure generation, it is necessary to isolate astrogliosis from other histopathological changes commonly associated with epilepsy (e.g. mossy fiber sprouting, granule cell dispersion, or loss of hilar neurons). We performed a detailed histological analysis on intraamygdaloid KA-injected or saline-injected mice. Three weeks following KA-injections, the ipsilateral amygdala and hippocampal injury sites were assessed for chronic histopathological alterations: Nissl staining confirmed the maintenance of the acute injury as evidenced by a profound loss of granular bodies within neurons located in the ipsilateral amygdala and hippocampus (Fig. 4A2 and B2, circles) compared to the respective contralateral structure (Fig. 4A1 and B1, circles). Importantly, however, no signs of granule cell dispersion, mossy fiber sprouting, or hilar cell loss were found (Fig. 4B) indicating that histopathological alterations commonly associated with epilepsy were lacking in our model.

The acute injuries in amygdala and CA3 were accompanied by a strong astrogliotic response identified by increased GFAP immunoreactive material within the ipsilateral amygdala and CA3 (Fig. 4A4 and B4, circles). We quantified the number of GFAP-positive cells in the affected amygdala or CA3 by cell counting (Li et al. 2008b) and compared these values with corresponding regions from the contralateral hemisphere ( $n = 6$ ); A significant increase of the number of GFAP-positive astrocytes within the ipsilateral amygdala ( $55.3 \pm 15.2$  vs  $17.1 \pm 7.1$  cells per section,  $n = 6$  mice, 2 sections each,  $T_{DF,10} = 5.56$ ,  $p < 0.001$ ) and CA3 ( $52.3 \pm 11.2$  vs  $15.6 \pm 4.3$  cells per section,  $n = 6$  mice, 2 sections each,  $T_{DF,10} = 7.45$ ,  $p < 0.001$ ) was identified. Furthermore, there were comparable numbers of GFAP-positive astrocytes between contralateral structures in the KA injected mice and control injected mice (amygdala,  $16.6 \pm 6.9$ ; CA3,  $14.5 \pm 3.6$ ). In accord with our previous findings (Aronica et al. 2011; Li et al. 2008a; Li et al. 2008b), the increase in astrogliosis was paralleled by a corresponding increase in ADK expression (Fig. 4A6 and B6, circles) which becomes readily apparent in higher magnification images (Fig. 4A8 and B8). Densitometry of ADK immunoreactive material was performed on scanned images acquired from the ipsi- and contralateral hemispheres of the amygdala and CA3 of KA injected mice ( $n = 6$  mice, 3 sections each). Compared to the contralateral hemisphere, ADK immunodensities were



increased by  $31.6 \pm 11.4\%$  in the amygdala ( $T_{DF,5} = 6.78$ ,  $p < 0.01$ ) and  $29.9 \pm 10.6\%$  in the CA3 ( $F_{2,15} = 14.29$ ,  $p < 0.001$ ). A low magnification image of a KA-injected brain showed that in regions outside of the CA3 and amygdala, such as the neocortex, ADK levels were comparable in both hemispheres (Fig. 5, circles demarcate the ipsilateral amygdala and CA3). This restricted pattern of injury and change in ADK expression within only the ipsilateral amygdala and CA3 was paralleled with GFAP expression as well (data not shown). Finally, we performed dual immunohistofluorescence with antibodies specific to GFAP and ADK to confirm that the upregulated ADK immunoreactive material was confined to reactive astrocytes (Fig. 6). Within both injury sites prominent astrogliosis (Fig. 6A2 and B2) and ADK overexpression (Fig. 6A4; 6B4) was evident. Furthermore, ADK was colocalized to astroglial cells in the ipsilateral amygdala and CA3 (Fig. 6A6 and B6). Conversely, the contralateral amygdala and hippocampus was spared from astrogliosis (Fig. 6A1 and B1) and ADK upregulation (Fig. 6A3 and B3). Thus, intraamygdaloid KA-induced SE resulted in chronic changes characterized by two distinct focal areas of astrogliosis and overexpression of ADK (in ipsilateral amygdala and CA3) in the absence of histopathological changes commonly associated with epilepsy.

### Focal electrographic seizures originate from discrete foci in amygdala and hippocampus

Since overexpression of ADK causes adenosine deficiency (Shen et al. 2011) and disrupted adenosine signaling increases the brain's susceptibility to seizures (Li et al. 2008b), we predicted that focal astrogliosis with overexpression of ADK as documented above is linked to seizures. To demonstrate a link between astrogliosis, increased levels of ADK, and seizures, it is necessary to document that seizures originate from focal areas of overexpressed ADK. We therefore performed synchronous EEG-recordings derived from multiple intracranial electrodes. If seizures originate from focal areas of overexpressed ADK, then seizures from two separate foci (amygdala and CA3) should be occurring independent from each other and should not spread to other brain areas, because adenosine homeostasis is expected to be intact outside those foci.

Mice injured with intraamygdaloid KA-induced SE were equipped with multiple bipolar EEG recording electrodes three weeks after injury to assess spontaneous electrographic activity in the amygdala and hippocampal formations. Electrodes were implanted into either the ipsilateral CA3/amygdala ( $n = 6$ ) or the ipsilateral CA1/CA3/dentate gyrus (DG) ( $n = 6$ ). Electrographic activity was compared with corresponding regions in control mice ( $n=4$ ). By first assessing the recordings from CA3/amygdala implanted mice we identified spontaneous focal seizures that independently originated from either the amygdala (Fig. 7B1) or from CA3 (Fig. 7B2) but never synchronized and never spread beyond these regions (Fig. 7B). The seizure activity in the amygdala consisted of high-voltage, polyspike paroxysmal discharges of  $>1$  Hz frequency with a clear beginning and followed by a post-ictal period (Fig. 7A). Furthermore, these seizures occurred at a rate  $3.9 \pm 1.3$  seizures per hour for an average duration of  $16.9 \pm 5.9$  seconds per seizure (based on 48 hours total recording time). For the current study we characterized 187 and 198 seizures in the amygdala and CA3, respectively, none of which occurred simultaneously. Given the rate and duration of the 385 spontaneous seizures, we calculated the probability that seizures simultaneously generate in the amygdala and CA3 is 1 out of 2,650 seizure events, and approximately 636 cumulative hours of EEG analysis would be necessary for this event to occur.

To address mechanistically, whether adenosine acting on adenosine  $A_1$  receptors ( $A_1R$ ) in non-injured brain region might prevent spread and synchronization of seizures, we performed pharmacological experiments using the  $A_1R$  antagonist 8-cyclopentyl-1,3-dipropylxanthine (DPCPX; 1 mg/kg i.p.). This dose of DPCPX does not trigger seizures in non-epileptic control animals, nor does it trigger seizures in animals with reduced seizure threshold, such as the rat kindling model (Masino et al. 2011; Szybala et al. 2009). Thus,

DPCPX is a highly specific pharmacological tool to tax the involvement of endogenous adenosine acting on A<sub>1</sub> receptors. After a single dose of DPCPX in intraamygdaloid KA-injected mice, spontaneous seizures immediately synchronized between CA3 and amygdala, and subsequently generalized to the cortex (Fig. 7B). These generalized electrographic seizures had a behavioral correlate that was equivalent to a stage 3 seizure on the Racine scale (head nodding, chewing, and generalized forelimb clonus) that was uniformly observed in each of the DPCPX-injected mice. In contrast, an equivalent injection of DPCPX into intraamygdaloid saline-injected control mice did not change the EEG pattern or cause any behavioral signs of a seizure (Fig. 7C). Immunohistochemistry performed after completion of EEG recording confirmed that ipsilateral amygdala and CA3 were characterized by astrogliosis and overexpressed ADK, but lacked any additional pathologies commonly associated with epilepsy (Fig. 4; Fig. 6).

### Spatial spread of focal seizures is prevented by adenosine

To assess whether *endogenous* adenosine – assumed to be unaltered outside the focal areas of astrogliosis-associated dysfunction of adenosine signaling – is responsible for preventing the spatial spread of focal seizures, we further characterized the electrographic activity throughout all the hippocampal subregions in mice implanted with electrodes into the CA1/CA3/DG. In agreement with our previous study (Li et al. 2008b) spontaneous seizures were confined to the CA3 subregion (Fig. 8B). The profile of the CA3-originating seizures (Fig. 8A) was remarkably similar to those of the amygdala in regards to the waveform, seizure rate ( $4.2 \pm 1.1$  seizures per hour with an average duration of  $18.1 \pm 4.6$  seconds per seizure) and response to DPCPX. Specifically, DPCPX caused the CA3-originating seizures to spread throughout the hippocampus to the CA1 and DG, and subsequently to the cortex (Fig. 8B). Those generalized seizures had a Racine stage 3 behavioral correlate as mentioned above. In contrast, seizures were never observed in amygdala, hippocampus, or cortex of saline-injected control mice (Fig. 8C) and DPCPX had no effect on the control EEG (Fig. 8C). These data demonstrate that focal disruption of adenosine homeostasis in CA3 triggers focal seizures restricted to CA3, but that *endogenous* adenosine, acting on A<sub>1</sub>Rs outside the CA3, prevents the spatial spread of seizures.

### Temporal spread of seizure intensity does not occur over several weeks

To determine if the seizure phenotype established 3 weeks after intraamygdaloid injection of KA is progressive over time, we compared ADK expression and electrographic seizure activity in the hippocampus two months after injection with respective data sets obtained at the three-week time point. First, we observed that the increase in ADK expression remained confined to the CA3 subregion (Fig 9B,D) and was similar to the staining pattern observed at three weeks (Fig. 4B6,8). Subsequent densitometry of ADK immunoreactive material 2 months after injury revealed a significant increase in ADK levels within the injured CA3 compared to the contralateral CA3 subregion ( $31.3 \pm 14.9\%$ ,  $F_{2,15} = 14.29$ ,  $p < 0.001$ ). However, there was not a significant difference between ADK levels at 3 weeks and 2 months after KA injection. Finally, analysis of electrographic activity from the CA3/CA1/DG demonstrate that spontaneous seizures remain confined to the CA3 (Fig. 9E) at a rate of  $4.4 \pm 1.5$  seizures per hour and average duration of  $19.7 \pm 7.1$  seconds per seizure. Comparison of these results with those from mice recorded three weeks after KA injection yielded no significant changes (rate,  $T_{DF,10} = 0.42$ ,  $p = 0.69$ ; duration,  $T_{DF,10} = 0.46$ ,  $p = 0.66$ ). These data demonstrate that in the absence of any other pathology commonly associated with epilepsy, the ADK-related seizure phenotype remains stable over time and does not seem to progress. Our DPCPX experiments (Fig. 7B; Fig. 8B) indicate that a secondary event is likely necessary to convert pre-existing ADK-related seizures into a clinical seizure phenotype.

## DISCUSSION

Multiple lines of evidence suggest that ADK is a molecular link between astrogliosis and increased neuronal excitability in epilepsy (Aronica et al. 2011; Gouder et al. 2004; Li et al. 2008b; Theofilas et al. 2011). Extracellular levels of adenosine are regulated largely by an astrocyte-based adenosine cycle and critically depend on expression levels of astrocytic ADK (Boison et al. 2010). Overexpression of ADK in astrogliosis leads to a reduction of intracellular levels of adenosine and therefore creates a 'sink' that drives the influx of extracellular adenosine via equilibrative nucleoside transporters into the astrocyte, thereby reducing the 'tone' of ambient adenosine leading to insufficient activation of adenosine receptors (Boison 2008). The focal origins of astrogliosis-associated seizures and mechanisms that govern their spread in space, time, and severity have not yet been investigated in a comprehensive manner. In the present communication, intraamygdaloid injection of the excitotoxin KA was used to trigger temporally restricted focal onset SE, in which subsequent astrogliosis was focal and isolated from histopathological changes commonly associated with epilepsy. Using this model we report here on several new findings that enhance our understanding of the role that astrogliosis and associated disruption of adenosine signaling plays within the context of seizure generation and spread. In particular we (i) report on a novel amygdala pathology characterized by focal astrogliosis, associated overexpression of ADK and focal subclinical seizures, (ii) demonstrate two independent seizure foci (in injured amygdala and ipsilateral CA3) that both express their own non-synchronized focal seizures, (iii) demonstrate spatial restriction of seizures to focal astrocytosis, (iv) demonstrate that spread of seizures outside those foci is inhibited by *endogenous* adenosine acting on A<sub>1</sub> receptors, (v) demonstrate that this seizure phenotype is stable over at least several weeks, and (vi) demonstrate that astrogliosis-associated ADK-related seizures are initially subclinical and require a second 'hit' (e.g. further compromise of adenosine signaling) to transform into generalized clinical seizures. Due to technical limitations (given the small size of the astroglial foci) in the present study it was not possible to quantify adenosine directly. Instead we used a pharmacological tool (DPCPX) and histological assessment of ADK expression levels as surrogate indicators for the tone of endogenous adenosine. The use of ADK as surrogate marker for the tone of ambient adenosine has been validated recently: *In vivo* quantification of adenosine with adenosine microelectrode biosensors performed in genetically engineered mice with regionally restricted expression changes in ADK have revealed that brain areas with genetically increased ADK expression (i.e. in striatum) or decreased ADK expression (i.e. in cerebral cortex), were characterized by significantly decreased and increased levels of adenosine, respectively (Shen et al. 2011). Several findings from our work warrant further discussion.

### Amygdala pathology

Intraamygdaloid KA-injection in rats or mice has widely been used as a model to study mechanisms of seizure-induced acute neuronal cell death in the hippocampal formation (Ben-Ari and Cossart 2000). Likewise, chronic responses to the acute injury have focused on the hippocampal formation (Li et al. 2008b). Here we provide the first comprehensive analysis of the amygdala pathology associated with this model of focal epileptogenesis. In particular, we demonstrate (i) acute neuronal cell loss (Fig. 2), (ii) astrogliosis and ADK overexpression that match the site of the original injury (Fig. 3 & 6), and (iii) spontaneous focal seizures that originate from the affected area (Fig. 7). Importantly, the histopathological alterations observed in amygdala (Fig. 2, 3, & 6) closely mimic those observed in the ipsilateral CA3 and result in a remarkably similar seizure phenotype in regards to both the rate (CA3:  $4.2 \pm 1.1$  vs. amygdala:  $3.9 \pm 1.3$  seizures per hour) and frequency (CA3:  $18.1 \pm 4.8$  vs. amygdala:  $16.9 \pm 5.9$  seconds). Our data are in line with findings from a neonatal rat model, in which KA injected into the amygdala of postnatal day



10 rat pups causes acute neuronal cell loss in amygdala followed by astrogliosis and spontaneous seizures in adulthood (Dunleavy et al. 2010). However, in the latter model astrogliosis was not isolated, but accompanied by additional pathological changes such as NPY expression and granule cell dispersion, resulting in an aggravated seizure phenotype (Dunleavy et al. 2010). Therefore, unlike our model, the contribution of astrogliosis to seizure generation could not be isolated.

### Focal origin of ADK-related seizures

Our findings demonstrate that within both the amygdala and hippocampus the same neuropathology of astrogliosis and ADK overexpression develops in parallel in response to SE (Fig. 4). Using multiple synchronous EEG recordings obtained simultaneously from different brain regions we were able to define the focal origin of astrogliosis-related seizures and to link them with overexpression of ADK ('ADK-related seizures'). In particular, we demonstrated that seizures in amygdala and CA3 are of independent origin (Fig. 7B). In >48 hours of cumulative EEG recording we never found seizures originating from either the amygdala or the CA3 to be synchronized. Remarkably, while seizures were recorded from either the amygdala or the CA3, seizure events were never recorded from any other region such as CA1, dentate gyrus, or cortex. Thus, seizures originated from two independent seizure foci (amygdala and CA3) and remained focal. Only after administration of the selective A<sub>1</sub>R antagonist DPCPX at a non-convulsive dose (non-epileptic control mice do not have any changes in their EEG-pattern as a response to DPCPX, Fig 7C, Fig. 8C) seizures synchronized between amygdala and CA3 (Fig. 7), and spread throughout the hippocampal formation and cortex resulting in convulsive stage 3 seizures. This finding is of interest, since the non-selective adenosine receptor antagonist caffeine is in widespread use among the epileptic population. However, any effects of caffeine differ between acute (pro-convulsive) and chronic (anti-convulsive) use (Boison 2010); importantly, chronic caffeine has been associated with a lowered susceptibility to pentylenetetrazol-induced seizures produced in mice, an effect that was dependent on the adenosine A<sub>2A</sub>R (El Yacoubi et al. 2008), a receptor with low expression levels in hippocampus, where it contributes to regulating neuronal activity (El Yacoubi et al. 2008), but high expression levels in striatum, where it contributes to psychomotor control (Shen et al. 2008). More research on the recreational or clinical use of adenosine receptor antagonists on seizure thresholds in susceptible populations is certainly warranted.

### Endogenous adenosine prevents seizure spread and generalization

As a potent antiepileptic (Boison 2005) and neuroprotectant (Cunha 2005) adenosine exerts its protective effects mainly by activation of the high affinity A<sub>1</sub>Rs. Activation of this receptor leads to inhibition of the presynaptic release of glutamate and stabilization of the postsynaptic membrane potential (Fredholm et al. 2005). The role of A<sub>1</sub>R-mediated inhibition in the regulation of seizure susceptibilities becomes evident in A<sub>1</sub>R knockout mice that have spontaneous electrographic seizures independent of additional injury (Li et al. 2008b; Masino et al. 2011). Here we demonstrate that intraamygdaloid KA injection caused two independent lesion sites that act as focal generators for spontaneous seizures that are electrographic. However, pharmacological manipulation of the endogenous adenosine system by blockade of A<sub>1</sub>Rs resulted in generalization beyond either the amygdala or CA3 to the cortex. These data indicate that systemic impairment of normal adenosine signaling is sufficient to permit the progression of pre-existing spontaneous electrographic seizures to a convulsive seizure phenotype. Therefore endogenous adenosine acting on A<sub>1</sub>Rs prevented seizure spread and generalization.

## Astrogliosis and epileptogenesis

Using a mouse model of intrahippocampal KA-induced SE, we previously identified astrogliosis and overexpression of ADK as part of a complex epileptic phenotype (Gouder et al. 2004), which also includes mossy fiber sprouting, granule cell dispersion, and hilar neuronal cell loss (Arabadzisz et al. 2005). Therefore, it was not possible to ascribe a specific function of astrocytes to seizure generation. In our present study, we were able to isolate astrogliosis from histopathological changes commonly associated with epileptogenesis and to demonstrate that astrogliosis in the absence of any additional component of the epileptogenic cascade is directly related to seizure generation and that disruption of adenosine homeostasis as part of the astrogliosis was associated with focal seizure initiation. The critical role of astrocytic ADK for seizure generation was recently confirmed by overexpressing ADK selectively in astrocytes using an adeno associated virus (AAV serotype 8) based vector. Otherwise healthy wild-type mice overexpressing the virus-induced ADK in astrocytes of the CA3 area of the hippocampal formation displayed the same kind of electrographic seizures reported here (Theofilas et al. 2011). These findings suggest that overexpression of ADK *per se* might be sufficient to trigger electrographic seizures. As a long-term response to acute injury, the adenosine system undergoes further changes that might eventually contribute to an aggravation of the seizure phenotype. Since we monitored our animals for not more than 2 months, we cannot exclude the possibility that the seizure phenotype described here may change over extended time periods. Thus, downregulation of A<sub>1</sub>Rs, which has been described in chronic epilepsy (Glass et al. 1996; Rebola et al. 2005), may serve as a mechanism that could turn pre-existing ADK-related seizures into an aggravated seizure phenotype.

### The relevance of ‘silent seizures’

Our data suggest that recurrent focal subclinical electrographic seizures are associated with a localized astrogliotic reaction that involves overexpression of ADK and resulting adenosine deficiency. It is important to note that seizures are frequent (about 4 per hour), relatively short (20 seconds), and subclinical. Under normal conditions these seizures appear to be stable over both space and time. Multiple pathological events can trigger focal astrogliosis; such triggers can range from minor traumatic injuries or micro-strokes – that might not even be noticed or detected – to pathologies with known involvement of astrogliosis, such as Alzheimer’s disease, autism, or amyotrophic lateral sclerosis (Rosengren et al. 1992; Schiffer and Fiano 2004; Van Eldik and Griffin 1994). Could it be that ‘silent seizures’ linked to astrogliosis and focal adenosine deficiency, are fairly widespread – if not common? If these seizures do not have a clinical manifestation, they will not necessarily be detected, but might still constitute a risk factor for subsequent seizure generalization and development of epilepsy. In support of this notion, patients with Alzheimer’s disease frequently suffer from episodes of sudden severe confusion that can best be explained by the occurrence of such ‘silent seizures’ in deep brain structures (Thomas, 1997). Furthermore, epileptic (clinical) seizures constitute a well-known comorbidity of Alzheimer’s. Thus, focal ADK-related seizures, as described here, might be the substrate for future seizure generalization and might constitute a first step in the epileptogenic cascade.

## Acknowledgments

This work was supported by grants R01NS065957, and R01NS061844, from the National Institutes of Health (NIH/NINDS).

## References

Arabadzisz D, Antal K, Parpan F, Emri Z, Fritschy JM. Epileptogenesis and chronic seizures in a mouse model of temporal lobe epilepsy are associated with distinct EEG patterns and selective

- neurochemical alterations in the contralateral hippocampus. *Exp Neurol*. 2005; 194(1):76–90. [PubMed: 15899245]
- Aronica E, Zurolo E, Iyer A, de Groot M, Anink J, Carbonell C, van Vliet EA, Baayen JC, Boison D, Gorter JA. Upregulation of adenosine kinase in astrocytes in experimental and human temporal lobe epilepsy. *Epilepsia*. 2011 [Epub ahead of print]. 10.1111/j.1528-1167.2011.03115.x
- Ben-Ari Y, Cossart R. Kainate, a double agent that generates seizures: two decades of progress. *Trends Neurosci*. 2000; 23(11):580–7. [PubMed: 11074268]
- Binder DK, Steinhäuser C. Functional changes in astroglial cells in epilepsy. *Glia*. 2006; 54(5):358–68. [PubMed: 16886201]
- Boison D. Adenosine and epilepsy: from therapeutic rationale to new therapeutic strategies. *Neuroscientist*. 2005; 11(1):25–36. [PubMed: 15632276]
- Boison D. The adenosine kinase hypothesis of epileptogenesis. *Progress in Neurobiology*. 2008; 84(3):249–262. [PubMed: 18249058]
- Boison D. Methylxanthines, seizures and excitotoxicity. *Handb Exp Pharmacol*. 2010; 200:251–266. [PubMed: 20859799]
- Boison D, Chen JF, Fredholm BB. Adenosine signalling and function in glial cells. *Cell Death Differ*. 2010; 17:1071–1082. [PubMed: 19763139]
- Boison D, Masino MA, Geiger JD. Homeostatic bioenergetic network regulation – a novel concept to avoid pharmacoresistance in epilepsy. *Expert Opinion on Drug Discovery*. 2011; 6(7):713–724. [PubMed: 21731576]
- Cunha RA. Neuroprotection by adenosine in the brain: from A1 receptor activation to A2A receptor blockade. *Purinergic Signaling*. 2005; 1:111–134.
- Dudek FE, Hellier JL, Williams PA, Ferraro DJ, Staley KJ. The course of cellular alterations associated with the development of spontaneous seizures after status epilepticus. *Prog Brain Res*. 2002; 135:53–65. [PubMed: 12143370]
- Dunleavy M, Shinoda S, Schindler C, Ewart C, Dolan R, Gobbo OL, Kerskens CM, Henshall DC. Experimental neonatal status epilepticus and the development of temporal lobe epilepsy with unilateral hippocampal sclerosis. *Am J Pathol*. 2010; 176(1):330–42. [PubMed: 19948825]
- Eid T, Williamson A, Lee TS, Petroff OA, de Lanerolle NC. Glutamate and astrocytes—key players in human mesial temporal lobe epilepsy? *Epilepsia*. 2008; 49(Suppl 2):42–52. [PubMed: 18226171]
- El Yacoubi M, Ledent C, Parmentier M, Costentin J, Vaugeois JM. Evidence for the involvement of the adenosine A(2A) receptor in the lowered susceptibility to pentylenetetrazol-induced seizures produced in mice by long-term treatment with caffeine. *Neuropharmacology*. 2008; 55(1):35–40. [PubMed: 18486156]
- Fredholm BB, Chen JF, Masino SA, Vaugeois JM. Actions of adenosine at its receptors in the CNS: Insights from knockouts and drugs. *Annu Rev Pharmacol Toxicol*. 2005; 45:385–412. [PubMed: 15822182]
- Glass M, Faull RL, Bullock JY, Jansen K, Mee EW, Walker EB, Synek BJ, Dragunow M. Loss of A1 adenosine receptors in human temporal lobe epilepsy. *Brain Res*. 1996; 710(1–2):56–68. [PubMed: 8963679]
- Gouder N, Scheurer L, Fritschy J-M, Boison D. Overexpression of adenosine kinase in epileptic hippocampus contributes to epileptogenesis. *J Neurosci*. 2004; 24(3):692–701. [PubMed: 14736855]
- Hinterkeuser S, Schroder W, Hager G, Seifert G, Blumcke I, Elger CE, Schramm J, Steinhäuser C. Astrocytes in the hippocampus of patients with temporal lobe epilepsy display changes in potassium conductances. *Eur J Neurosci*. 2000; 12(6):2087–96. [PubMed: 10886348]
- Li T, Lan JQ, Boison D. Uncoupling of astrogliosis from epileptogenesis in adenosine kinase (ADK) transgenic mice. *Neuron Glia Biology*. 2008a; 4(2):91–99. [PubMed: 19674507]
- Li T, Ren G, Lusardi T, Wilz A, Lan JQ, Iwasato T, Itohara S, Simon RP, Boison D. Adenosine kinase is a target for the prediction and prevention of epileptogenesis in mice. *J Clin Inv*. 2008b; 118(2):571–582.
- Masino SA, Li T, Theofilas P, Sandau US, Ruskin DN, Fredholm BB, Geiger JD, Aronica E, Boison D. A ketogenic diet suppresses seizures in mice through adenosine A1 receptors. *J Clin Inv*. 2011; 121(7):2679–2683.

- Pascual O, Casper KB, Kubera C, Zhang J, Revilla-Sanchez R, Sul JY, Takano H, Moss SJ, McCarthy K, Haydon PG. Astrocytic purinergic signaling coordinates synaptic networks. *Science*. 2005; 310(5745):113–6. [PubMed: 16210541]
- Pignataro G, Simon RP, Boison D. Transgenic overexpression of adenosine kinase aggravates cell death in ischemia. *J Cereb Blood Flow Metab*. 2007; 27(1):1–5. [PubMed: 16685255]
- Racine R. Kindling: the first decade. *Neurosurg*. 1978; 3(2):234–252.
- Rebola N, Porciuncula LO, Lopes LV, Oliveira CR, Soares-da-Silva P, Cunha RA. Long-term effect of convulsive behavior on the density of adenosine A1 and A 2A receptors in the rat cerebral cortex. *Epilepsia*. 2005; 46(Suppl 5):159–65. [PubMed: 15987272]
- Rosengren LE, Ahlsen G, Belfrage M, Gillberg C, Haglid KG, Hamberger A. A sensitive ELISA for glial fibrillary acidic protein: application in CSF of children. *J Neurosci Methods*. 1992; 44(2–3): 113–9. [PubMed: 1474847]
- Rouach N, Koulakoff A, Abudara V, Willecke K, Giaume C. Astroglial metabolic networks sustain hippocampal synaptic transmission. *Science*. 2008; 322(5907):1551–5. [PubMed: 19056987]
- Schiffer D, Fiano V. Astrogliosis in ALS: possible interpretations according to pathogenetic hypotheses. *Amyotroph Lateral Scler Other Motor Neuron Disord*. 2004; 5(1):22–5. [PubMed: 15204020]
- Seifert G, Carmignoto G, Steinhauser C. Astrocyte dysfunction in epilepsy. *Brain Res Rev*. 2010; 63(1–2):212–21. [PubMed: 19883685]
- Shen H-Y, Coelho JE, Ohtsuka N, Canas PM, Day Y-J, Huang Q-Y, Rebola N, Yu L, Boison D, Cunha RA, et al. A critical role of the adenosine A2A receptor in extra-striatal neurons in modulating psychomotor activity as revealed by opposite phenotypes of striatum- and forebrain-A2A receptor knockouts. *J Neurosci*. 2008; 28(12):2970–2975. [PubMed: 18354001]
- Shen HY, Lusardi TA, Williams-Karnesky RL, Lan JQ, Poulsen DJ, Boison D. Adenosine kinase determines the degree of brain injury after ischemic stroke in mice. *J Cereb Blood Flow Metab*. 2011; 31(7):1648–1659. [PubMed: 21427729]
- Studer FE, Fedele DE, Marowsky A, Schwerdel C, Wernli K, Vogt K, Fritschy JM, Boison D. Shift of adenosine kinase expression from neurons to astrocytes during postnatal development suggests dual functionality of the enzyme. *Neuroscience*. 2006; 142(1):125–37. [PubMed: 16859834]
- Szybala C, Pritchard EM, Wilz A, Kaplan DL, Boison D. Antiepileptic effects of silk-polymer based adenosine release in kindled rats. *Exp Neurol*. 2009; 219:126–135. [PubMed: 19460372]
- Theofilas P, Brar S, Stewart K-A, Shen H-Y, Sandau US, Poulsen DJ, Boison D. Adenosine kinase as a target for therapeutic antisense strategies in epilepsy. *Epilepsia*. 2011; 52(3):589–601. [PubMed: 21275977]
- Van Eldik LJ, Griffin WS. S100 beta expression in Alzheimer's disease: relation to neuropathology in brain regions. *Biochim Biophys Acta*. 1994; 1223(3):398–403. [PubMed: 7918676]
- Wilz A, Pritchard EM, Li T, Lan JQ, Kaplan DL, Boison D. Silk polymer-based adenosine release: Therapeutic potential for epilepsy. *Biomaterials*. 2008; 29(26):3609–3616. [PubMed: 18514814]

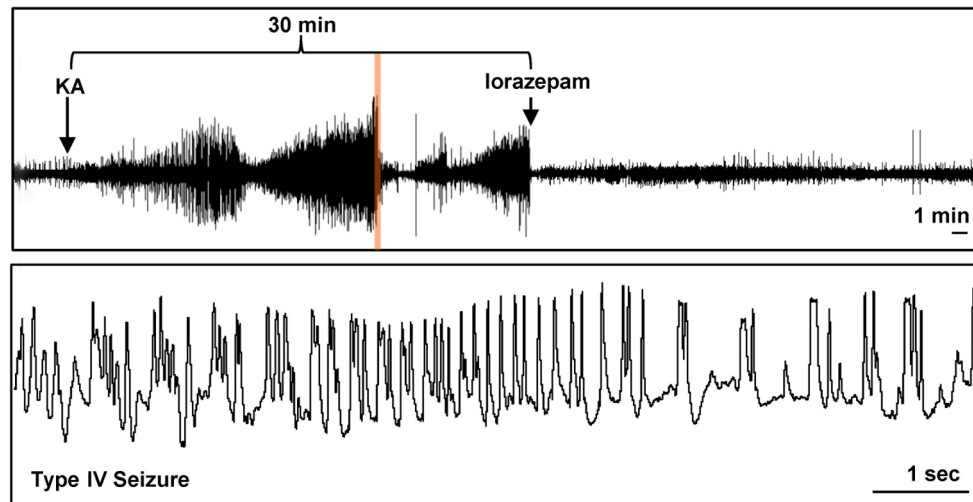


**Figure 1.** Intraamygdaloid injection of KA induces status epilepticus. The upper trace is a representative 60 minute cortical EEG recording that includes the 30 minute period of status epilepticus terminated by lorazepam injection. The lower trace is a high resolution 10 sec segment obtained from the upper trace (demarcated by orange highlight) that is an example of type IV seizure activity.



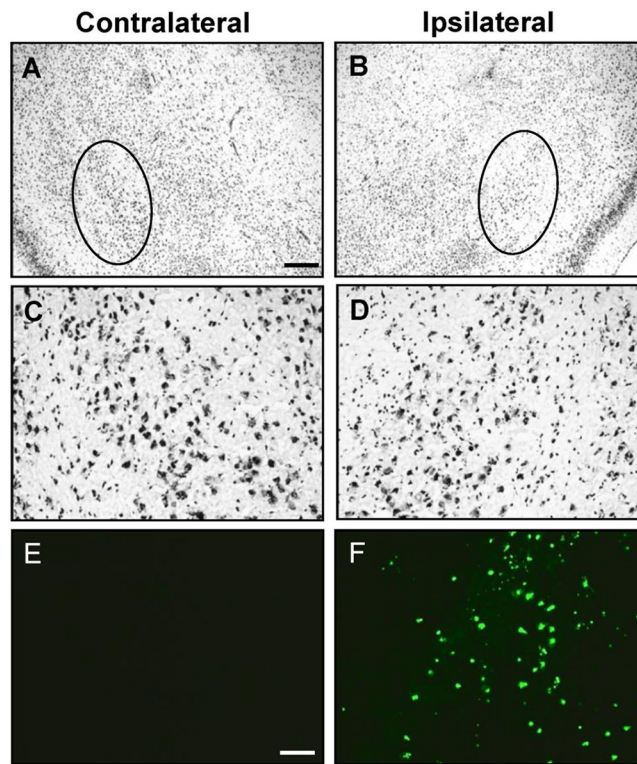


**Figure 2.** Intraamygdaloid KA injection induces acute cell death within the ipsilateral amygdala. A–D, Representative images of Nissl staining in the contra- (A,C) and ipsilateral (B,D) amygdala 24 hours after intraamygdaloid KA injection. A,B, Disrupted Nissl staining in the ipsilateral amygdala (B, circle) and the corresponding unaffected contralateral region (A, circle). C,D, Higher magnification images of the Nissl stained regions demarcated by circles in panels A and B, respectively. E,F, TUNEL labeling of sections adjacent to panels A and B. Scale bars: 300  $\mu\text{m}$  (AD), 75  $\mu\text{m}$  (E–F).

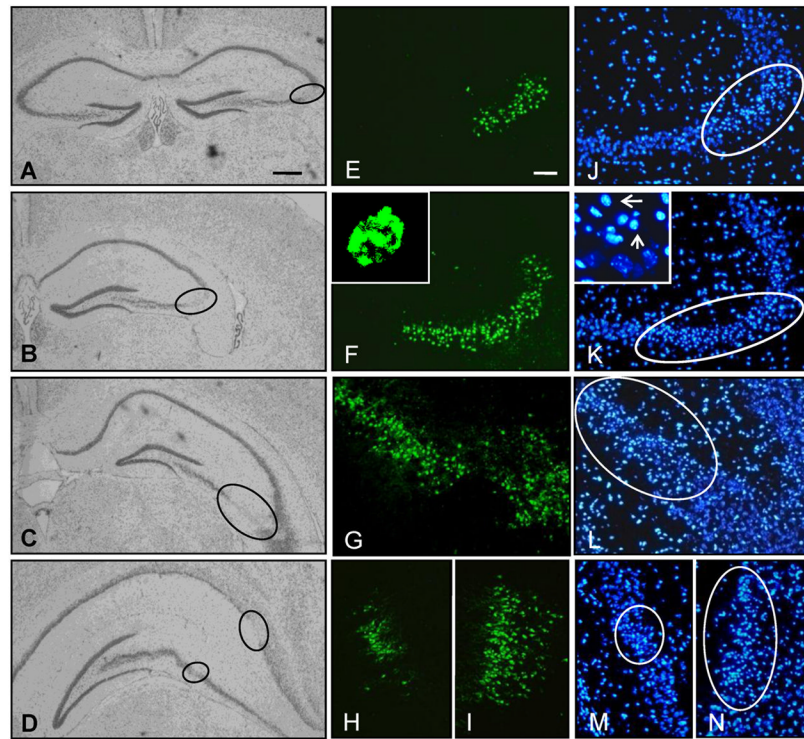


**Figure 3.** A single focal intraamygdaloid KA injection causes acute cell death that is restricted to the CA3. A–D, Representative Nissl stained sections showing CA3 selective damage (circles) throughout the rostral-caudal extent of the hippocampus 24 hours post intraamygdaloid KA-injection. E–N, Representative images of TUNEL labeled cells (E–I) and DAPI stained nuclei (J–N) that correspond to the respective areas demarcated by circles in panels A–D. Insets depict TUNEL labeling (F) and DAPI staining (K, arrows) of condensed nuclei. Scale bars: 300  $\mu\text{m}$  (A–D), 75  $\mu\text{m}$  (E–N).

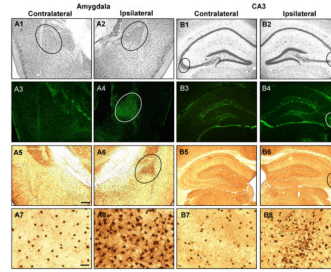


**Figure 4.**

Intraamygdaloid KA injection causes chronic injury associated with astrogliosis and ADK overexpression in the ipsilateral amygdala and CA3. A1,2;B1,2, Representative Nissl staining of the injured (A2, B2; circles) and corresponding non-injured (A1, B1; circles) amygdala (A1,2) and CA3 (B1,2) 3 weeks after KA injection. A3-8;B3-8, Representative images of GFAP (A3,4;B3,4) and ADK (A5-8;B5-8) immunoreactive material in the amygdala (A3-8) and CA3 (B3-8). Increased GFAP (A4,B4; circles) and ADK (A6,B6; circles) immunoreactive material is only present in the ipsilateral injury site and correspond to disrupted Nissl staining. A7,8;B7,8, High magnification images obtained from the contralateral amygdala (A7) and CA3 (B7) and within the area demarcated by circles in panels A6 and B6 for the ipsilateral amygdala (A8) and CA3 (B8), respectively. Scale bars: 300  $\mu\text{m}$  (A1-6;B1-6), 37.5  $\mu\text{m}$  (A7,8;B7,8).

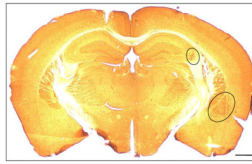


**Figure 5.** Chronic injury from intraamygdaloid KA injection causes brain region-specific changes in ADK expression levels. Low magnification image of ADK immunoreactive material in a coronal brain section from a KA injected mouse three weeks after SE. The circles demarcate the ipsilateral amygdala and CA3 regions which have increased ADK expression in comparison to the corresponding contralateral regions. Scale bar: 500  $\mu$ m.

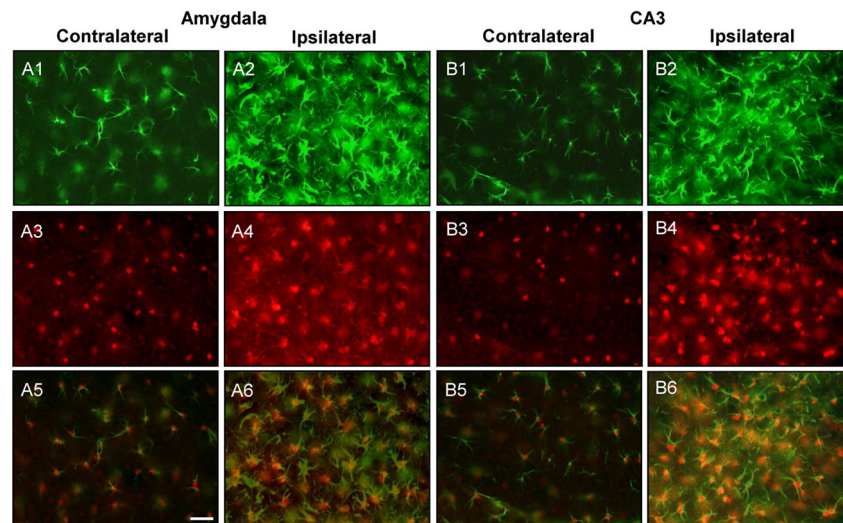


**Figure 6.** ADK upregulation colocalizes with astrogliosis in the injured amygdala and CA3. A1-4;B1-4, Representative images of GFAP (A1,2;B1,2, green) and ADK (A3,4;B3,4, red) double labeled sections that were acquired from within the amygdala and CA3 three weeks after intraamygdaloid KA injection. The ipsilateral amygdala (A2,4) and CA3 (B2,4) have increased GFAP (green) and ADK (red) immunoreactive material compared to the contralateral hemispheres (A1,3;B1,3). A5,6;B5,6, Merged fluorescence image of GFAP and ADK immunoreactive material. The increased levels of ADK immunoreactive material (red) colocalizes with reactive astrocytes (GFAP, green) within the ipsilateral amygdala (A6) and CA3 (B6). Scale bars: 37.5  $\mu$ m (A1-6;B1-6).



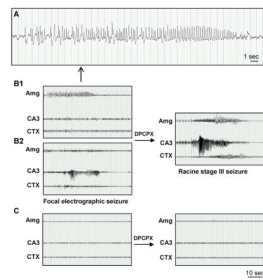


**Figure 7.**

Focal spontaneous seizures develop in the amygdala and CA3 three weeks after intraamygdaloid KA injection. A, High resolution EEG trace of the amygdala-originating spontaneous focal electrographic seizure depicted in panel B1. B, Recordings three weeks after KA injection from bipolar electrodes implanted into the amygdala (Amg) and CA3 and from a monopolar electrode implanted in the cortex (CTX). Note that spontaneous electrographic seizures are focal, but alternate in origin between the Amg (B1) and CA3 (B2). DPCPX injection (1 mg/kg in 20% DMSO/saline, i.p) synchronizes electrographic seizure activity in the Amg and CA3 with subsequent generalization to the CXT (right). C, Recordings from the Amg, CA3 and CTX in control saline-injected mice. Note that there was no response to DPCPX (right). Scale bars: 1 second (A); 10 seconds (B,C).

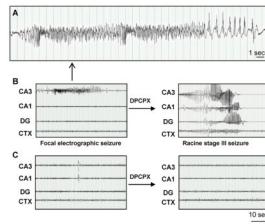


**Figure 8.**

Spontaneous electrographic seizures in the hippocampus are confined to the CA3 subregion. A, High resolution EEG trace of the CA3-originating spontaneous focal electrographic seizure depicted in panel B. B, Recordings three weeks after KA injection from bipolar electrodes implanted into the CA1/CA3/dentate gyrus (DG) and monopolar electrode in the cortex (CTX). DPCPX injection (1 mg/kg, i.p) generalizes electrographic seizure activity throughout the hippocampus and into the CTX (right). C, Recordings from the CA3/CA1/DG and CTX in control saline-injected mice. Note that there was no response to DPCPX (right). Scale bars: 1 second (A); 10 seconds (B,C).

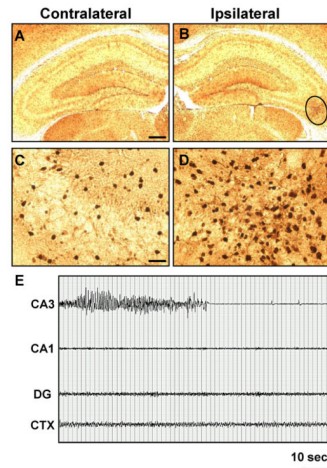


**Figure 9.** Hippocampal damage from intraamygdaloid KA is persistent. A–D, ADK immunoreactive material in the contralateral (A,C) and ipsilateral (B,D) CA3 two months after KA injection. E, Recordings from mice implanted with bipolar electrodes into the CA3/CA1/dentate gyrus (DG) and reference electrode into the cortex (CTX) two months after KA injection. Note that spontaneous electrographic seizure activity is localized to the CA3 subregion. Scale bars: 300  $\mu\text{m}$  (A, B), 37.5  $\mu\text{m}$  (C,D).